Development 129, 455-466 (2002)
Printed in Great Britain © The Company of Biologists Limited 2002
DEV1754

Pax6 is required to regulate the cell cycle and the rate of progression from symmetrical to asymmetrical division in mammalian cortical progenitors

Guillermo Estivill-Torrus[1,*], Helen Pearson[2,*], Veronica van Heyningen[2], David J. Price[1,†] and Penny Rashbass[2,3,†]

[1]Department of Biomedical Sciences, University of Edinburgh Medical School, Hugh Robson Building, George Square, Edinburgh EH8 9XD, UK
[2]MRC Human Genetics Unit, Western General Hospital, Crewe Road, Edinburgh EH4 2XU, UK
[3]Centre for Developmental Genetics, Department of Biomedical Science, University of Sheffield, Firth Court, Western Bank, Sheffield S10 2TN, UK

*These authors contributed equally to the work

†Authors for correspondence (p.rashbass@sheffield.ac.uk and dprice@ed.ac.uk)

Accepted 24 October 2001

SUMMARY

In the proliferative zone of the developing cerebral cortex, multipotential progenitors predominate early in development and divide to increase the progenitor pool. As corticogenesis progresses, proportionately fewer progenitors are produced and, instead, cell divisions yield higher numbers of postmitotic neurones or glial cells. As the switch from the generation of progenitors to that of differentiated cells occurs, the orientation of cell division alters from predominantly symmetrical to predominantly asymmetrical. It has been hypothesised that symmetrical divisions expand the progenitor pool, whereas asymmetrical divisions generate postmitotic cells, although this remains to be proved. The molecular mechanisms regulating these processes are poorly understood.

The transcription factor Pax6 is highly expressed in the cortical proliferative zone and there are morphological defects in the *Pax6*$^{Sey/Sey}$ (*Pax6* null) cortex, but little is known about the principal cellular functions of Pax6 in this region. We have analysed the cell-cycle kinetics, the progenitor cleavage orientation and the onset of expression of differentiation markers in *Pax6*$^{Sey/Sey}$ cortical cells in vivo and in vitro. We showed that, early in corticogenesis at embryonic day (E) 12.5, the absence of Pax6 accelerated cortical development in vivo, shortening the cell cycle and the time taken for the onset of expression of neural-specific markers. This also occurred in dissociated culture of isolated cortical cells, indicating that the changes were intrinsic to the cortical cells. From E12.5 to E15.5, proportions of asymmetrical divisions increased more rapidly in mutant than in wild-type embryos. By E15.5, interkinetic nuclear migration during the cell cycle was disrupted and the length of the cell cycle was significantly longer than normal in the *Pax6*$^{Sey/Sey}$ cortex, with a lengthening of S phase.

Together, these results show that Pax6 is required in developing cortical progenitors to control the cell-cycle duration, the rate of progression from symmetrical to asymmetrical division and the onset of expression of neural-specific markers.

Key words: Cerebral cortex, Cortical plate, *Pax6*, Small eye, Mouse, Cell cycle, Cell proliferation, Asymmetrical cell division, p27^{Kip1}, Ventricular zone

INTRODUCTION

The adult neocortex (hereafter called the cortex) is composed of six radial layers of neurones, each defined by cellular morphology, cell density and the formation of distinct axonal connections. During development, cortical cells are generated in the pseudostratified epithelium that forms the ventricular zone (VZ), a layer of dividing progenitor cells at the inner (ventricular) surface of the dorsal telencephalon (Sauer, 1935; Sidman et al., 1959; Bayer and Altman, 1991; Takahashi et al., 1993; Takahashi et al., 1995a; Takahashi et al. 1995b). As progenitor cells progress through the cell cycle their nuclei undergo dynamic intracellular migration, termed interkinetic nuclear migration. During this process, nuclei move away from the apical surface during G1, occupy the basal half of the VZ during S phase and return apically in G2 so that mitosis occurs at the ventricular surface (Sidman et al., 1959; Fujita, 1964).

Retroviral lineage tracing experiments have revealed multipotent progenitors in the mammalian VZ (Luskin et al., 1988; Price and Thurlow, 1988; Walsh and Cepko, 1992; Grove et al., 1993). At least some multipotent progenitors are thought to be self-renewing stem cells (Temple and Davis, 1994; Reid et al., 1995; Williams and Price, 1995; Qian et al., 1998) that predominate early in development (Williams and Price, 1995; Qian et al., 1998). It has been hypothesised that they are produced by progenitors dividing symmetrically, in a plane

roughly at right angles to the ventricular surface (also known as vertical cleavage) to produce two identical daughter cells that remain within the VZ, thus expanding the proliferative population. As cortical neurogenesis progresses, asymmetrical division, which occurs in a plane roughly parallel to the ventricular surface (also known as horizontal cleavage), starts to predominate. It has been hypothesised that asymmetrical division produces two different daughter cells, one that remains within the VZ as a progenitor and one that migrates away from the VZ to differentiate (Kornack and Rakic, 1995; Chenn and McConnell, 1995; Doe, 1996; Mione et al., 1997; Lu et al., 2000; Matsuzaki, 2000). Although these hypotheses are attractive, there is no direct proof that the symmetry of division predicts the fates of the daughter cells in this way.

In the mouse cortex, neurones are generated between embryonic day (E) 12.5 and E17.5 (Gillies and Price, 1993) and the VZ is eventually lost at around birth. Cortical progenitors undergo a maximum of 11 cell cycles during neurogenesis (Takahashi et al., 1995b) and the laminar identity of cortical neurones is closely correlated to the cell cycle in which the cell is born. Thus, neurones of layers 6 and 5 arise from cycles 1-8 in mice, whereas neurones destined for layers 4 and 3/2 are born in cycles 9-11 (Takahashi et al., 1996). The layers of the cortex are, therefore, formed in an inside-first, outside-last sequence by migration of neurones from the VZ.

The mechanisms that regulate the cell cycle of cortical progenitors and the transition from predominantly symmetrical to predominantly asymmetrical divisions in the VZ as cortical neurogenesis proceeds are poorly understood. We present evidence that the transcription factor Pax6 is involved in the regulation of this progression. *Pax6* encodes two DNA-binding motifs, a paired domain (Bopp et al., 1986; Treisman et al., 1991) and a paired-like homeodomain (Frigerio et al., 1986). *Pax6* expression in the mouse embryo begins at E8.0 in the anterior surface ectoderm and neuroepithelium of the closing neural tube in the presumptive spinal cord, forebrain and hindbrain (Walther and Gruss, 1991; Stoykova and Gruss, 1994; Grindley et al., 1995). As the forebrain develops, *Pax6* expression becomes restricted to specific telencephalic regions, including the VZ of the developing cortex, where it persists throughout corticogenesis, and specific diencephalic regions (Walther and Gruss, 1991; Stoykova and Gruss, 1994; Grindley et al., 1995; Grindley et al., 1997; Stoykova et al., 1996; Caric et al., 1997; Mastick et al., 1997; Warren and Price, 1997). Homozygous $Pax6^{Sey/Sey}$ embryos, lacking any functional Pax6 protein, fail to develop eyes and nasal cavities, exhibit brain abnormalities and die soon after birth (Hogan et al., 1986; Hill et al., 1991; Schmahl et al., 1993; Stoykova et al., 1996; Warren and Price, 1997; Grindley et al., 1997; Mastick et al., 1997). Abnormalities of the forebrain arise as early as E9.5 when the region of the prosencephalon giving rise to the cerebral vesicles shows altered morphology (Mastick et al., 1997). Previous single-pulse bromodeoxyuridine (BrdU) labelling studies have suggested that defects in the cell cycle of $Pax6^{Sey/Sey}$ cortical and diencephalic progenitors might underlie some of these abnormalities (Warren and Price, 1997; Gotz et al., 1998; Warren et al., 1999).

We analysed the distribution and cleavage orientation of mitotic cells and the production of postmitotic cells in the $Pax6^{Sey/Sey}$ cortex during neurogenesis. We found that proportions of asymmetrically dividing cells increased more rapidly than normal from E12.5 to E15.5 and that newborn cells expressed neural-specific markers sooner after their generation. To assess how these observations relate to progression through the cell cycle, we performed cumulative BrdU labelling. At E12.5 the length of the cell cycle in the mutant was approximately 60% of that in wild-type littermates. To test whether this was an intrinsic property of mutant cortical cells, we cultured E12.5 dissociated $Pax6^{Sey/Sey}$ cortical cells in isolation. These cells displayed increased proliferation rates compared with wild-type cells and an accumulation of the cyclin-dependent kinase inhibitor protein $p27^{Kip1}$. This protein has been shown to be necessary for the timing of cell-cycle withdrawal that precedes terminal differentiation (Casaccia-Bonnefil et al., 1997; Durand et al., 1997; Durand et al., 1998; Borriello et al., 2000; Levine et al., 2000; Miyazawa et al., 2000; Sasaki et al., 2000). However, although the cell cycle was shortened early in corticogenesis in $Pax6^{Sey/Sey}$ embryos, we found that, later in development, proliferation was slowed. Analysis of progenitors in older cortex (E15.5) showed that the length of the cell cycle increased to over 140% of that in wild-type littermates, with a large increase in the length of S phase in the mutant cortex.

MATERIALS AND METHODS

Mice

All mouse embryos were derived from $Pax6^{SeyEd}$ heterozygote crosses (referred to as $Pax6^{Sey}$; also called Sey^{Ed}) (Roberts, 1967) maintained on an outbred CD1 background. The mutation in $Pax6^{SeyEd}$ is G194X, which is predicted to result in a truncated nonfunctional protein lacking the homeodomain and C-terminal sequences (Hill et al., 1991). The day of the vaginal plug following mating was designated E0.5. Pregnant females were killed by cervical dislocation.

Histological analysis of cell division

To obtain a complete representation of cell division patterns throughout the developing cortex, a comprehensive count of cells in telophase was undertaken. Experiments were performed at three ages: E10.5, E12.5 and E15.5. Whole embryos at E10.5 and E12.5 and brains at E15.5 were dissected into cold phosphate buffer, fixed in 4% paraformaldehyde in phosphate-buffered saline (PBS) overnight and washed 3×5 minutes in 4% sucrose in PBS at room temperature. Tissues were embedded in melted 1.5% agar, 5% sucrose in PBS, transferred to 30% sucrose in PBS and left at 4°C until the blocks sank (usually 2 days). Blocks were rapidly frozen on dry ice and 10 μm coronal cryostat sections were cut, defrosted at room temperature for at least 30 minutes and processed for immunohistochemistry as described in Zhong et al. (Zhong et al., 1996). Antibodies used were against Numblike (Zhong et al., 1997) (rabbit polyclonal, 1:1000 dilution; generous gifts from W. Zhong and Y. N. Jan), phosphorylated histone H3 (Hendzel et al., 1997) (rabbit polyclonal, 1:2000 dilution, Upstate Biotechnology, NY) and Pax6 (Kawakami et al., 1997) (mouse monoclonal, 1:100, Developmental Studies Hybridoma Bank (DSHB), University of Iowa). After secondary labelling with fluorescent conjugated antibodies (Jackson Laboratories, PA), slides were washed three times in PBS and mounted in Vectashield (Vector Laboratories, UK) containing 1 μg/ml 4,6-diamidino-2-phenylindole (DAPI, Molecular Probes, Eugene). Images were taken with a Xillix Microimager 1400 CCD camera on a Zeiss Axioplan II microscope using IPLab (Scanalytics). For the analysis of cell division patterns, two wild-type and two $Pax6^{Sey/Sey}$ embryos for each age were sectioned. At least 180 cells in the proliferative zones in each brain were assessed as shown in Fig. 1; numbers of cells undergoing ectopic

division, symmetrical division, asymmetrical division or intermediate division were counted. Each data set was shown to comply with the assumptions necessary for ANOVA.

Determination of cell-cycle kinetics in vivo

Analysis of cell-cycle kinetics in the cortex of E12.5 and E15.5 wild-type and *Pax6$^{Sey/Sey}$* embryos was performed as described by Nowakowski et al. (Nowakowski et al., 1989). In brief, BrdU pulses (70 μg/g body weight, i.p.) were given to pregnant dams every 2 hours for up to 8 hours (at E12.5) or for up to 12 hours (at E15.5). Dams at age E12.5 were killed 0.5, 2.5, 4.5 and 8.5 hours after the first injection. Dams at E15.5 were killed 0.5, 4.5, 8.5 and 12.5 hours after the first injection. The embryos were fixed for 3 hours in 4% paraformaldehyde, wax-embedded and processed to reveal BrdU immunoreactivity as described elsewhere (Gillies and Price, 1993). Parasagittal sections, 10 μm, were cut. The proportions of cells in the proliferative zone that were BrdU labelled were counted in 100 μm wide strips through the depth of the cortex at the rostral pole, the caudal pole and centrally in three nonadjacent sections that cut through the full rostrocaudal extent of the cortex. We found no consistent differences in the proportions of labelled cells (termed the labelling index, LI) rostrally, caudally and centrally and so data from the three sampling points were combined to give mean LIs and standard errors. For each age, we obtained data from two embryos for each timepoint and plotted data for each animal separately against the length of exposure to BrdU.

For double-labelling studies, after BrdU detection the sections were washed in PBS and incubated overnight in neurone-specific anti-β tubulin isotope III (TuJ1; mouse monoclonal, dilution 1:400, Sigma). The second antibody was detected using an alkaline phosphatase conjugated rabbit mouse IgG (Sigma) and 4-nitro blue tetrazolium chloride/5-bromo-4-chloro-3-indolyl-phosphate (Roche). Five hundred rostral, 500 caudal and 500 centrally positioned cells (1500 in total) from nonadjacent sections were counted. Again, we found no consistent differences in the counts from each location and data from the three regions in each animal were combined.

Culture experiments

Cells from E12.5 cortices were dissociated by incubation for 45 minutes at 37°C in Earle's buffered salts solution containing papain (20 units/ml; Papain Dissociation System, Worthington Biochemical, UK). Cells in suspension were plated onto poly-L-lysine-coated wells (LabTek II™; Nunc Life Technologies, UK) at a density of 1.5×10^5 cells/cm^2 and cultured in defined serum-free medium (Romijn et al., 1994) at 37ºC and 5% CO_2. Cultures were analysed at various times after plating (12.75-24 hours, see below) and each time-point was repeated in three separate experiments. Viable cells were identified on the basis of morphology and exclusion of Trypan Blue. For cell counts, between 800 and 1500 viable cells per culture were assessed in five or six randomly selected microscope fields.

Twelve hours after plating, BrdU was added to the culture medium (final concentration 10 μM) and, after 45 minutes, BrdU was removed and fresh culture medium was added. Cells were fixed in 4% paraformaldehyde either immediately after the pulse of BrdU, i.e. 12.75 hours after plating, or at 15, 18, 21 and 24 hours after plating, washed in PBS, and processed for BrdU incorporation as described previously (Shetty and Turner, 1998). Monoclonal anti-BrdU (clone BU 33, Sigma, UK) was used at 1:1000 dilution.

Other immunocytochemical reactions were carried out as follows. All steps were at room temperature. Cultures were treated with 90% methanol prior to incubation in blocking solution (PBS containing 0.5% Triton X-100 and 2.5% normal rabbit serum). Cells were then exposed to one of the following monoclonal antibodies for 18 hours: anti-p27^{Kip1} (mouse monoclonal, 1:1000, Transduction Laboratories, NJ); anti-cyclin A (mouse monoclonal, 1:1000, Sigma, UK); anti-MAP2 (microtubule associated protein 2; mouse monoclonal, 1:400, Sigma, UK); TuJ1 (mouse monoclonal, 1:400, Sigma, UK); glial cell marker RC2 (mouse monoclonal, 1:50, DSHB, University of Iowa); anti-nestin rat 401 (mouse monoclonal, 1:100, DSHB, University of Iowa); anti-GFAP (glial fibrillary acidic protein; mouse monoclonal, 1:400, Sigma, UK); and anti-CNPase (2-′,3′-cyclic nucleotide-3′-phosphodiesterase; mouse monoclonal, 1:500, Sigma, UK). Subsequent processing was with biotin conjugated rabbit anti-mouse Ig (IgM for RC2) (1:400, both from Dako, UK) for 2 hours and ExtrAvidin®-peroxidase (1:500 in PBS, Sigma, UK) for 20 minutes. The reactions were developed with 3,3′- diaminobenzidine (DAB, Sigma, UK). All antibodies were diluted in blocking solution. Omission of the primary antibody resulted in no detectable staining.

For dual-labelling experiments, after developing in DAB, cultures were washed and exposed to 90% methanol to inhibit the peroxidase activity due to the first immunostaining. Wells were washed and processed for the second staining using the procedure described above. However, to distinguish the brown product from first reaction, the second staining was visualised with a blue reaction product using tetramethylbenzidine as substrate (HistoMark TrueBlue®, Kirkegaard and Perry Laboratories, UK).

Statistical analysis

For both sectioned material and cell culture experiments, data sets were compared by ANOVA (statistical significance between data sets was assigned when $P<0.05$).

RESULTS

Interkinetic nuclear migration and cleavage orientations are disrupted in the *Pax6$^{Sey/Sey}$* cerebral cortex

In vivo analyses were performed at E10.5, E12.5 and E15.5, which correlate with the onset of cortical neurogenesis, early neurogenesis and mid-neurogenesis (Gillies and Price, 1993; Caviness et al., 1995; Price et al., 1997). Cells in metaphase were visualized using an antibody directed against phosphorylated histone H3. This antibody binds weakly within pericentromeric heterochromatin during G2 and then spreads in an ordered fashion coincident with mitotic chromosome condensation, becoming strongest during metaphase (Hendzel et al., 1997). In wild-type cortex at all three ages metaphase cells were largely restricted to the ventricular surface, as expected (Fig. 1C). This was also the case in *Pax6$^{Sey/Sey}$* cortex at E10.5 and E12.5, but at E15.5 there appeared to be a significant proportion of metaphase cells located ectopically, away from the ventricular edge (Fig. 1D).

Quantification gave a more comprehensive representation of cell-division patterns throughout the developing cortex. Sections were stained with DAPI, which clearly identifies cells in late anaphase and telophase when condensed chromosomes are separating, and the number of cells in these stages were counted. In each section (n=15 per brain), cells throughout the depth of the cortical proliferative zone were simultaneously classified by position, either at the ventricular surface or ectopic (within the proliferative zone but more than three cell diameters from the ventricular surface) (Fig. 1C,D); or by orientation of division, either symmetrical (plane of division at 90º±30º to the ventricular surface), asymmetrical (parallel, 0°±30º, to ventricular surface) or intermediate (30-60º or 120-150º) (Fig. 1E-G). The spindles of cortical progenitors rotate throughout metaphase but stop at the start of anaphase (Adams, 1996) and so this method provides an accurate measure of the plane of division. It has been shown that the distributions of

cleavage orientations observed by staining fixed sections are identical to those observed by following living cells in cortical slices (Chenn and McConnell, 1995). The cortex exhibits temporal gradients of development; for example, anterior cortex is more mature than posterior cortex at any given stage of corticogenesis (Bayer and Altman, 1991). To test whether cell division patterns were influenced by the anterior-posterior gradient of development, counts were carried out on five adjacent sections at three different anterior-posterior positions in the cortex: 25%, 50% and 75% through the telencephalon (where 0% is the most rostral part and 100% is the most caudal: Fig. 1A,B). Position was found to have no significant effect on the incidence of either ectopic or asymmetrical division and data from the different regions were combined in the final analyses.

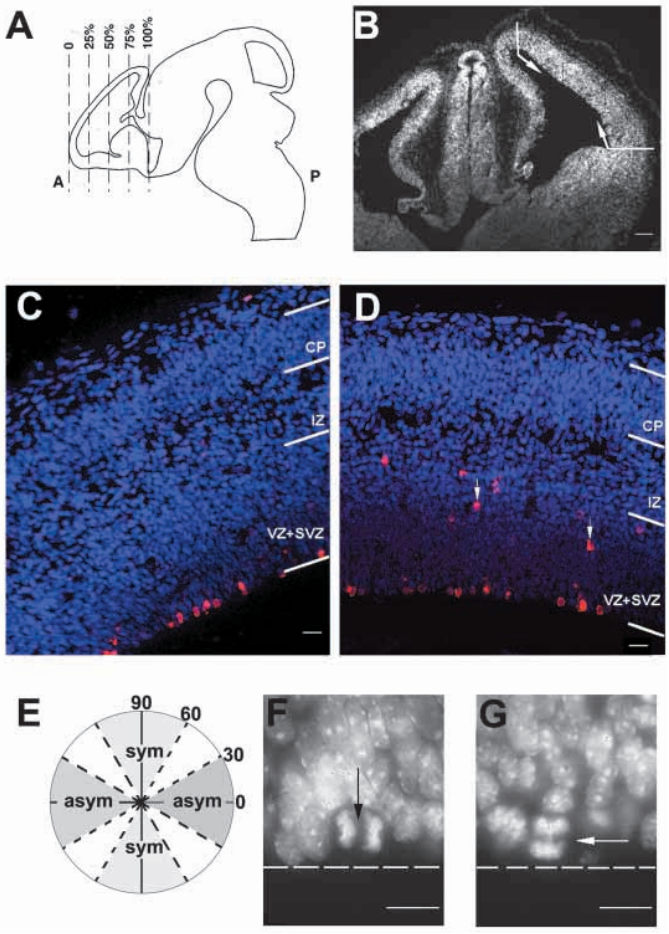

Fig. 1. Counting parameters used for in vivo analysis.
(A) Parasagittal view of an E12.5 wild-type forebrain showing the planes of section in which cell divisions were counted. Cells were counted in five sections at 25%, 50% and 75% through the telencephalon (broken lines). (B) Coronal section through an E12.5 wild-type embryo at a position 50% through the telencephalon (dorsal is upwards). Cell nuclei are stained with DAPI. Cell counts were made in the ventricular zone of the cortex between the two arrows. (C,D) Mitotic cells in (C) wild-type and (D) *Pax6*$^{Sey/Sey}$ E15.5 cortex identified with an antibody against phosphorylated histone H3, which labels metaphase chromosomes. In the wild-type cortex the majority of dividing cells are located at the ventricular surface; in the *Pax6*$^{Sey/Sey}$ cortex some dividing cells are located ectopically (away from the ventricular surface, arrows). (E) Late anaphase and telophase cells were classified by their plane of division relative to the ventricular surface (0°): –30° to 30°, asymmetrical division; 30° to 60°, intermediate division; 60° to 120°, symmetrical division. (F,G) DAPI-labelled chromosomes showing (F) symmetrical and (G) asymmetrical cell divisions. Broken line indicates plane of ventricular surface and arrow indicates plane of cell division. CP, cortical plate; IZ, intermediate zone; VZ, ventricular zone. Scale bars: 100 μm in B; 20 μm in C,D; 5 μm in F,G.

ANOVA revealed that the proportions of dividing cells located ectopically was significantly higher in *Pax6*$^{Sey/Sey}$ cortex than in wild-type cortex specifically at E15.5 (Fig. 2A). At E10.5, 3% of wild-type and 7% of *Pax6*$^{Sey/Sey}$ divisions were ectopic. This proportion rose slightly at E12.5 to 12% in wild-type and 17% in *Pax6*$^{Sey/Sey}$ cortex. At E15.5, only 13% of divisions occurred ectopically in wild-type compared with 47% in *Pax6*$^{Sey/Sey}$ embryos (P<0.005). These data strongly suggest that interkinetic nuclear migration is disrupted by mid-neurogenesis, perhaps because cells enter mitosis before or after their nuclei undergo apical relocation to the ventricular surface.

The analysis of cleavage orientations revealed that the proportions of cells undergoing asymmetrical division in the *Pax6*$^{Sey/Sey}$ cortex progressed to higher levels more rapidly than in wild-type cortex (Fig. 2B,C). In the E10.5 and E12.5 wild-type cortex (Fig. 2B), the majority of divisions (almost 80%) were symmetrical; the rest were almost equally divided between asymmetrical and intermediate. By E15.5, the proportion of symmetrical divisions had fallen by about 10%, whereas the proportion of asymmetrical divisions had risen by a similar amount (Fig. 2B). These data are consistent with a predicted increase in proportions of asymmetrical divisions as neurogenesis progresses (Chenn and McConnell, 1995). In the *Pax6*$^{Sey/Sey}$ cortex at E10.5, the distribution of cleavage orientations was close to that observed in wild-type littermates, although the proportion of symmetrical divisions was slightly lower and that of asymmetrical divisions was correspondingly higher than in wild-types (Fig. 2C). This difference from wild-type cortex became progressively more pronounced with age. By E12.5 the proportion of asymmetrical divisions was up to 17±2% (compared with 8±2% in wild-types; P<0.05); by E15.5, 36±2% of divisions occurred asymmetrically (compared with 17±2% in wild-types; P<0.0005) and only 48±2% were dividing symmetrically (Fig. 2C). The proportions of intermediate cells remained at similar levels throughout in both genotypes (Fig. 2B,C). These data indicate that the change towards asymmetrical division is accelerated in the *Pax6*$^{Sey/Sey}$ cortex as compared with wild-type cortex.

Cell-cycle kinetics are disrupted during development of the *Pax6*$^{Sey/Sey}$ cortex

To investigate further the kinetics of the cell cycle in the ventricular zone of mutant and wild-type embryos, E12.5 and E15.5 pregnant dams were given repeated injections of BrdU to label cumulatively the proliferating population. The proportions of BrdU-labelled cells in the proliferating zone after different times of exposure to BrdU are plotted in Fig. 3A,B. Using the model described by Nowakowski et al. (Nowakowski et al., 1989), and used since by others (Takahashi et al., 1993; Takahashi et al., 1995a; Takahashi et al., 1995b; Takahashi et al., 1996), these data can be interpreted as summarised in Fig. 3C to give the proportion of cells in the proliferative zone that are actually proliferating (i.e. the growth

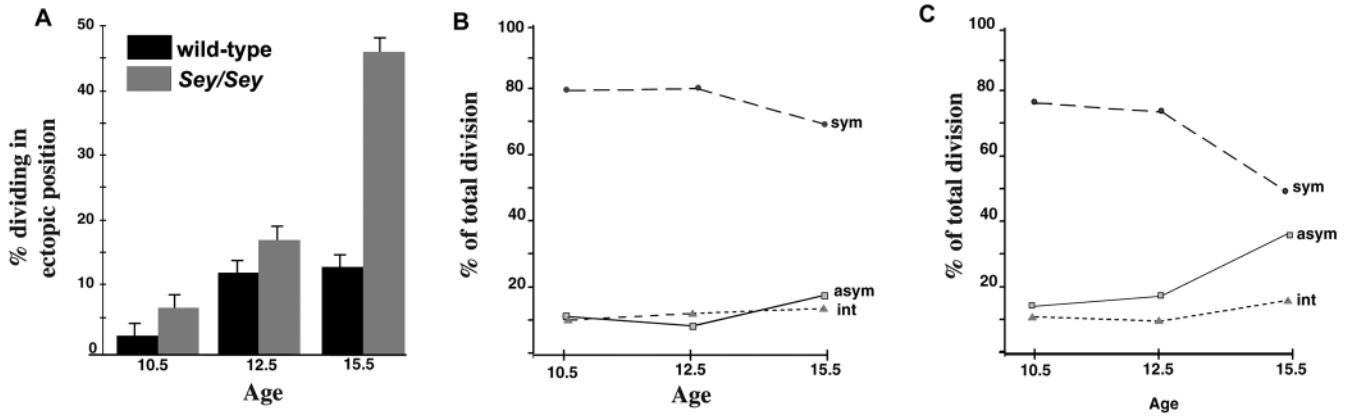

Fig. 2. Analysis of ectopic cell division and distribution of cleavage orientation in wild-type and *Pax6*$^{Sey/Sey}$ cortex at E10.5, E12.5 and E15.5. (A) Histogram showing the mean percentage (±s.e.m.) of late anaphase and telophase cells that are dividing in an ectopic postion (away from the ventricular surface) in wild-type cortex and *Pax6*$^{Sey/Sey}$ cortex. There is an increase in ectopic division at E15.5 in the mutants(P<0.0005). (B,C) Graphs comparing the mean percentages of dividing cells undergoing symmetrical, asymmetrical and intermediate division in (B) wild-type and (C) *Pax6*$^{Sey/Sey}$ cortex. All data points are ±2%.

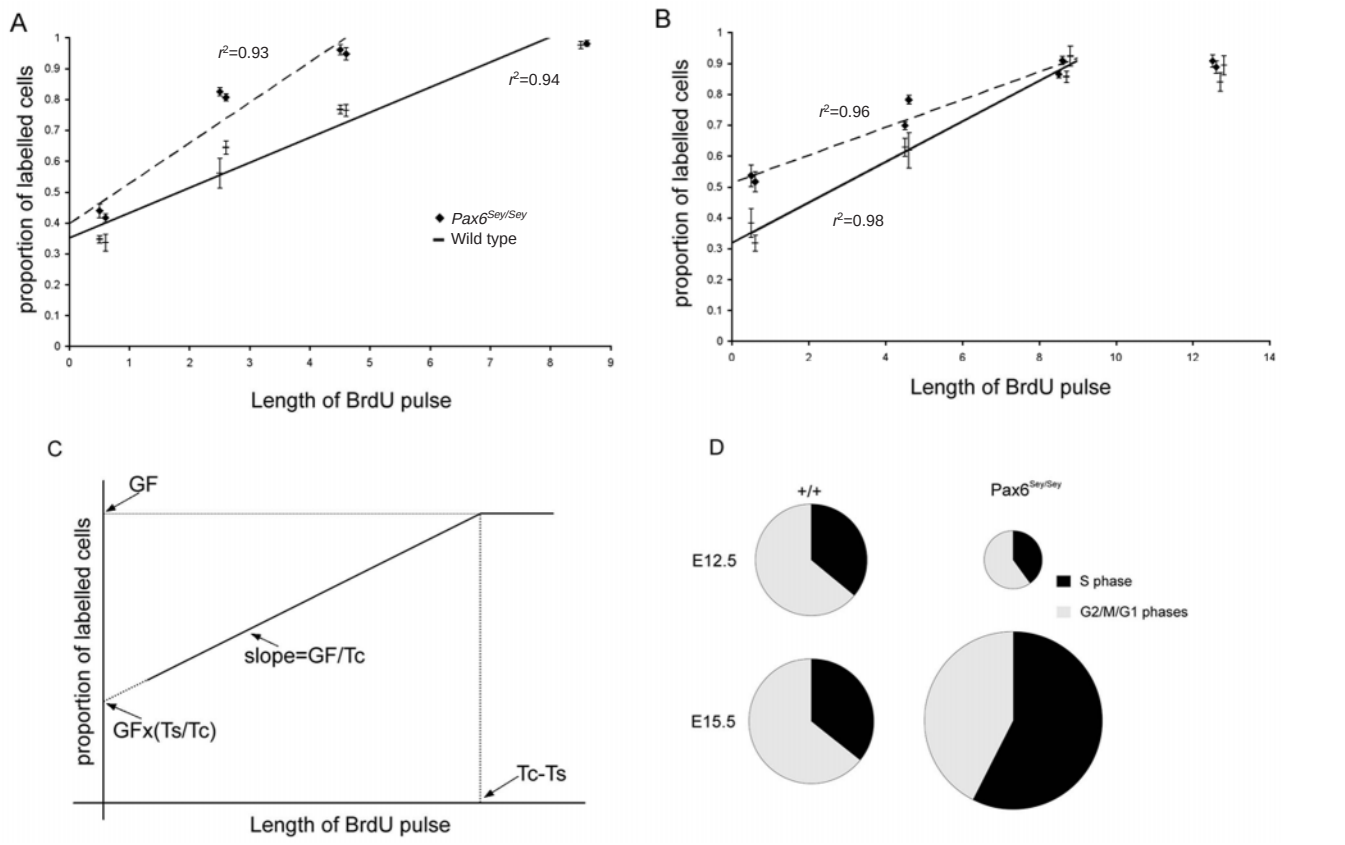

Fig. 3. Analysis of cell-cycle kinetics. (A,B) Graphs show results of cumulative labelling with BrdU at (A) E12.5 and (B) E15.5 in *Pax6*$^{Sey/Sey}$ and wild-type embryos, following the approach described by Nowakowski et al. (Nowakowski et al., 1989). Data points are means±s.e.m. of the proportions of BrdU-labelled cells in the cortex of each embryo. The proportions increased over 4.5 hours in E12.5 *Pax6*$^{Sey/Sey}$ embryos (broken line in A) and over 8-8.5 hours in all other cases. Least squares fit analysis of these rising phases (i.e. excluding data after giving 8.5 hours of BrdU to *Pax6*$^{Sey/Sey}$ embryos aged E12.5 and after giving 12.5 hours of BrdU to embryos of both genotypes aged E15.5) yielded the trendlines and r^2 values shown. (C) The growth fraction (GF), the length of S phase (Ts) and the length of the cell cycle (Tc) are calculated using the equations of Nowakowski et al. (Nowakowski et al., 1989). The intercept on the y-axis=GF×(Ts/Tc); the time where the GF is maximal (Tm)=Tc-Ts; the rate of increase (i.e. the slope) of the proportion of labelled cells=GF/Tc. (D) Cell-cycle kinetics in wild-type and mutant telencephalon at E12.5 and E15.5. The circumference of each circle is proportional to the overall length of the cell cycle at the different stages. The wild-type cell cycle lengthens slightly between E12.5 and E15.5. In the mutant, overall cell-cycle length is significantly shorter than normal at E12.5 and longer than normal at E15.5. The proportion of time that the cells spend in S phase is not significantly different between mutant cortex and wild-type cortex at E12.5. However, by E15.5 the proportion of time in S phase is markedly increased in the mutant.

fraction, GF), the length of the cell cycle (Tc) and the length of S phase (Ts).

Growth fractions were almost 1.0 at E12.5 and approximately 0.9 at E15.5, irrespective of genotype (Fig. 3A,B). The length of the cell cycle in E12.5 mutants was 60% that of wild-type littermates (7.5 hours for *Pax6*$^{Sey/Sey}$, 12.5 hours for wild-type). The length of S-phase was approximately 3 hours in mutants and approximately 4.5 hours in wild-types; these values represent 40% and 36% of the lengths of their respective cell cycles. Our values for Tc and Ts in E12.5 wild-type telenlencephalon were very close to those found before in E12-E13 mouse cortex (Takahashi et al., 1995b). In E15.5 wild-type cortex, the length of the cell cycle had increased, as described previously (Takahashi et al., 1995b). However, although the cell cycle was around 14 hours in wild-type embryos, it had increased to over 20 hours in mutant brains. Even more surprisingly, we found that, although Ts in the wild-type cortex remained almost constant (4.5 hours at E12.5 and 5 hours at E15.5, i.e. constantly 36% of the total cell cycle), Ts in the mutant increased dramatically from 3 hours (40% of the total cell cycle) at E12.5 to 11.5 hours (58% of the total cell cycle) at E15.5. Thus, although at E12.5 mutant cell cycles are much shorter, both wild-type and mutant cells spend similar proportions of time in S phase. By contrast, by E15.5 mutant cell cycles are longer and mutant cells spend a much greater proportion of time in S phase (summarized in Fig. 3D).

The expression patterns of TuJ1 and Numblike are altered in *Pax6*$^{Sey/Sey}$ cortex

The cell-division analysis described above revealed that the proportion of cells undergoing asymmetrical division in the *Pax6*$^{Sey/Sey}$ cortex progressed to higher levels more rapidly than their wild-type littermates. It has been suggested that asymmetrical divisions generate postmitotic neurones (Chenn and McConnell, 1995), although this hypothesis has not been proved directly. We tested whether cells switch on neural-specific markers earlier in the mutant cortex than in the wild-type cortex. We performed double labelling for BrdU and TuJ1 expression in sections from pregnant dams aged E12.5 and E15.5 that had been injected with BrdU at two hourly intervals for up to 8 and 12 hours, respectively. These animals were killed at 2.5 hours (E12.5 dams only), 4.5 hours (E12.5 and E15.5 dams), 8.5 hours (E12.5 and E15.5 dams) and 12.5 (E15.5 dams only) after the initial administration of BrdU. The percentages of the BrdU-labelled cells that were also labelled for TuJ1 were counted in the VZ. Within each of the four groups of animals defined according to age and genotype (E12.5 wild-type; E12.5 mutant; E15.5 wild-type; E15.5 mutant), the proportions of BrdU-labelled cells within the VZ that were also TuJ1 positive remained comparatively constant with increasing length of exposure to BrdU. This was presumably because the generation of new TuJ1-positive cells would be counterbalanced by the migration of older TuJ1-positive cells out of the VZ, as it has previously been observed that migration from the mutant VZ occurs at a normal rate at the ages studied here (Caric et al., 1997). There were, however, major differences between the groups such that only 2.5±0.6% of BrdU-labelled cells within E12.5 wild-type VZ were double-labelled cells (Fig. 4A), whereas 21.2±2.7% of BrdU-positive VZ cells were double labelled in the mutant (Fig. 4B). At E15.5, 6.4±3.9% of BrdU-labelled cells were

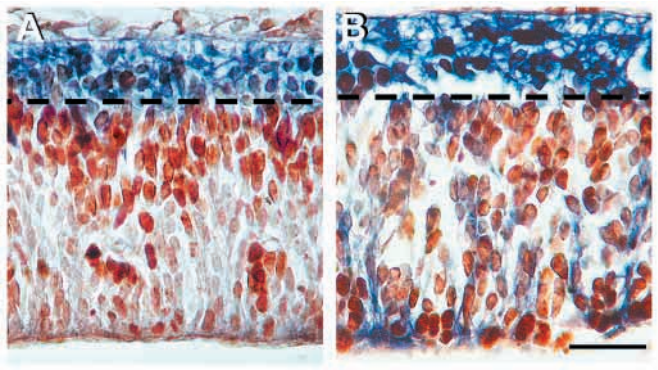

Fig. 4. Expression of BrdU and TuJ1 in wild-type and *Pax6*$^{Sey/Sey}$ E12.5 cortex. Parasagittal sections through cortex of (A) wild-type and (B) *Pax6*$^{Sey/Sey}$ E12.5 telencephalon. Dams were injected at 0 and 2 hours and embryos collected at 2.5 hours after initial injection. Broken line indicates boundary of VZ. There is a clear increase in double-labelled cells (BrdU, brown; TuJ1, purple) in the mutant (B) compared with the wild-type (A) littermate. Scale bar: 60 μm.

double labelled in the wild-type VZ, compared with 51.2±9.3% in the mutant VZ. These data indicate that the time between S phase and the onset of expression of neural specific markers is significantly shorter than normal in the *Pax6*$^{Sey/Sey}$ cortex.

We also tested the possibility that the expression of other cell fate determinants normally associated with postmitotic neurones might be increased in *Pax6*$^{Sey/Sey}$ cortex. In wild-type mice, Numblike (Nbl) is expressed in postmitotic cortical neurones but not in progenitors in the ventricular zone (Zhong et al., 1997). We examined the expression of Nbl in *Pax6*$^{Sey/Sey}$ cortex at E10.5-E15.5 (Fig. 5).

At E10.5 the developing telencephalic wall consists almost entirely of proliferating neuroepithelial cells, and nuclear staining with Pax6 antibody was evident in the majority of these cells in wild-type embryos (Fig. 5B). The antibody did not detect Pax6 protein in *Pax6*$^{Sey/Sey}$ mutant embryos (Fig. 5E,K). Cytoplasmic Nbl expression was detected in the emerging preplate, or primordial plexiform layer, of the cortex in both E10.5 wild-type and E10.5 *Pax6*$^{Sey/Sey}$ telencephalon (Fig. 5C,F). The preplate is formed by the first postmitotic cells migrating from the VZ (Marin-Padilla, 1998). More Nbl-positive cells were apparent in the *Pax6*$^{Sey/Sey}$ preplate (Fig. 5F) than in the wild-type preplate (Fig. 5C). By E15.5 the developing wild-type cortex has a well-defined laminar structure comprising proliferative layers (ventricular zone, VZ and subventricular zone, SVZ), an intermediate layer (IZ) of radially migrating neurones, and differentiating neurones and afferent and efferent axons in the cortical plate (CP). Expression of Pax6 was detected in the VZ and SVZ of the wild-type cortex (Fig. 5H). Intense Nbl immunoreactivity was seen in the nonproliferative layers of the cortex of both wild-type and *Pax6*$^{Sey/Sey}$ embryos (Fig. 5I,L). Unlike earlier ages, it was hard to assess numbers of labelled cells at E15.5, but in the *Pax6*$^{Sey/Sey}$ cortex there was an overall upregulation of Nbl immunostaining in the cortical plate relative to that in the IZ (Fig. 5L). These findings support the notion that neurogenesis is more advanced in the mutants at both early and intermediate stages of corticogenesis.

E12.5 *Pax6*$^{Sey/Sey}$ dissociated cortical cells show increased proliferation and terminal differentiation in culture

Because the *Pax6*$^{Sey/Sey}$ embryo has numerous abnormalities of tissues surrounding and interacting with cortex, we tested whether alterations of the cell cycle and rates of differentiation in the cortex are an intrinsic property of mutant cortical cells by growing these cells in isolation in culture. Dissociated E12.5 cortical cells were plated and, 12 hours later, a pulse of BrdU was added for 45 minutes. Cultures were studied 12.75, 15, 18, 21 and 24 hours after plating. We characterised the behaviour of cells and their expression of molecular markers in the cultures after staining with a range of antibodies. We did not observe any significant level of cell death in either wild-type or *Pax6*$^{Sey/Sey}$ cultures at any time-point. Although the two genotypes were plated at the same density, the mutant cells became increasingly clustered together compared with the wild-type cells (Fig. 6A,B). Cells labelled with BrdU were found in all cultures at all time-points. Fig. 6A-D shows BrdU labelling 24 hours after plating (i.e. 11.25 hours after the end of the BrdU pulse). At this stage, the latest that we studied, the wild-type BrdU-labelled cells remained either single or in small clusters containing less than 12 cells connected by a network of cellular processes (Fig. 6A,C). By contrast, *Pax6*$^{Sey/Sey}$ cells were clustered into much larger groups of up to 50 cells (Fig. 6B,D) and their nuclei often displayed a chain-like morphology (Fig. 6D), similar to that described previously (Gotz et al., 1998).

To characterise further the cells in the cultures, we used antibodies against specific cell markers including TuJ1 (Lee et al., 1990; Easter et al., 1993) and MAP2 (Matus, 1991) for neurones, GFAP for astrocytes (Dahl, 1981), CNPase for oligodendrocytes (Sprinkle et al., 1987), RC2 for radial glia (Misson et al., 1988) and nestin for undifferentiated neural precursors (Lendahl et al., 1990). Throughout the culture period, we detected predominantly neuronal cell markers (nestin, TuJ1 and MAP2) in both mutant and wild-type cells (Fig. 6A,B,E-H). The marker RC2 was also detected in cells of both genotypes (Fig. 6I,J), but very few mutant or wild-type cells were positive for GFAP or CNPase (data not shown). Many of the RC2-positive cells co-expressed MAP2 (Fig. 6I,J), in line with recent findings that radial glial cells may generate neurones (Barres, 1999; Malatesta et al., 2000).

We followed the proliferative behaviour of the cultured cells quantitatively by measuring, at a series of times after administration of BrdU, the proportions of BrdU-positive cells, the overall densities of cells in the culture, the proportions of cells containing the nuclear

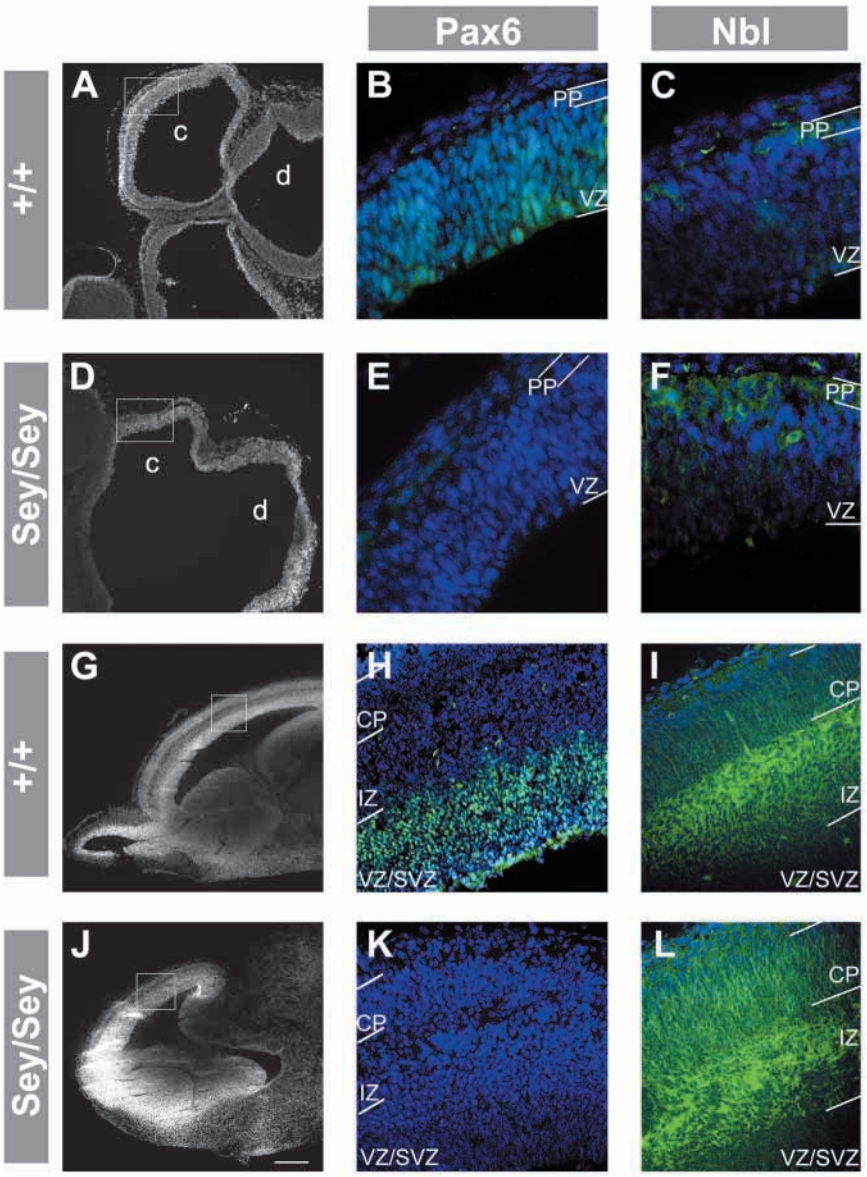

Fig. 5. Expression of Pax6 and Numblike (Nbl) in wild-type and *Pax6*$^{Sey/Sey}$ cortex. In all sections dorsal is upwards and in colour images nuclei are counterstained with DAPI (blue). (A-F) Coronal sections through (A-C) E10.5 wild-type and (D-F) E10.5 *Pax6*$^{Sey/Sey}$ brains. (G-L) Parasagittal sections through (G-I) E15.5 wild-type and (J-L) E15.5 *Pax6*$^{Sey/Sey}$ brains. (A,D,G,J) Low-magnification images of (A,G) wild-type and (D,J) *Pax6*$^{Sey/Sey}$ brain sections stained with DAPI. Boxes show areas in the cortex in which images to right were taken. (B,E,H,K) Nuclear Pax6 expression (green) is detected in wild-type ventricular zone (B,H) but not in the mutant (E,K). (C,F,I,L) Weak cytoplasmic Nbl expression (green) is detected in a few cells in E10.5 wild-type preplate (PP) (C). The Nbl expression domain has expanded in the wild-type cortex by E15.5 (I): expression is observed in both the wild-type intermediate zone (IZ) and cortical plate (CP), although expression levels appear to be much stronger in the IZ compared with the CP. (F,L) In the mutant, more Nbl-positive cells are detected in the preplate at E10.5 (F) compared with wild type (C). Nbl is highly expressed by cells in the *Pax6*$^{Sey/Sey}$ IZ and CP at E15.5 (L). The Nbl expression appears higher in the mutant CP compared with wild-type levels. c, cerebral vesicle; d, diencephalon; SVZ, subventricular zone, VZ, ventricular zone. Scale bars: 100 μm in A,D; 10 μm in B,C,E,F,H,I,K,L; 200 μm in G,J.

protein, cyclin A, which is expressed selectively during the S/G2/M phases of the cell cycle (Darzynkiewicz et al., 1996), and the proportions of cells expressing p27^{Kip1}, a cyclin-dependent kinase inhibitor that is required for neuronal cells to exit the cell cycle and start terminal differentiation (Sherr and Roberts, 1995; Sherr and Roberts, 1999; Casaccia-Bonnefil et al., 1997; Durand et al., 1997; Durand et al., 1998; Borriello et al., 2000; Levine et al., 2000; Miyazawa et al., 2000; Sasaki et al., 2000). Results are shown in Fig. 7. Immediately after the pulse of BrdU, the proportion of BrdU-labelled mutant cells was approximately twice that of the wild-type cells (Fig. 7A), indicating that proliferation rates are increased in *Pax6*$^{Sey/Sey}$ cortical cells in vitro as well as in vivo. In wild-type cultures, the proportions of BrdU-labelled cells increased over the following 8.25 hours, as the cells that had been in S-phase during the pulse of BrdU underwent division, and fell again over the next 3 hours, presumably as proliferating cells that had not been labelled by the BrdU pulse divided to dilute the BrdU-labelled population (Fig. 7A). The schematic in Fig. 8A illustrates this course of events. In stark contrast, the proportions of BrdU-labelled mutant cells increased steadily throughout culture (Fig. 7A). This observation, together with our finding that overall cell density increased more rapidly in the cultures of mutant cells than in the cultures of wild-type cells (Fig. 7B), suggests that mutant cells continued to proliferate more rapidly than wild-type cells for up to 24 hours in culture (Fig. 8B).

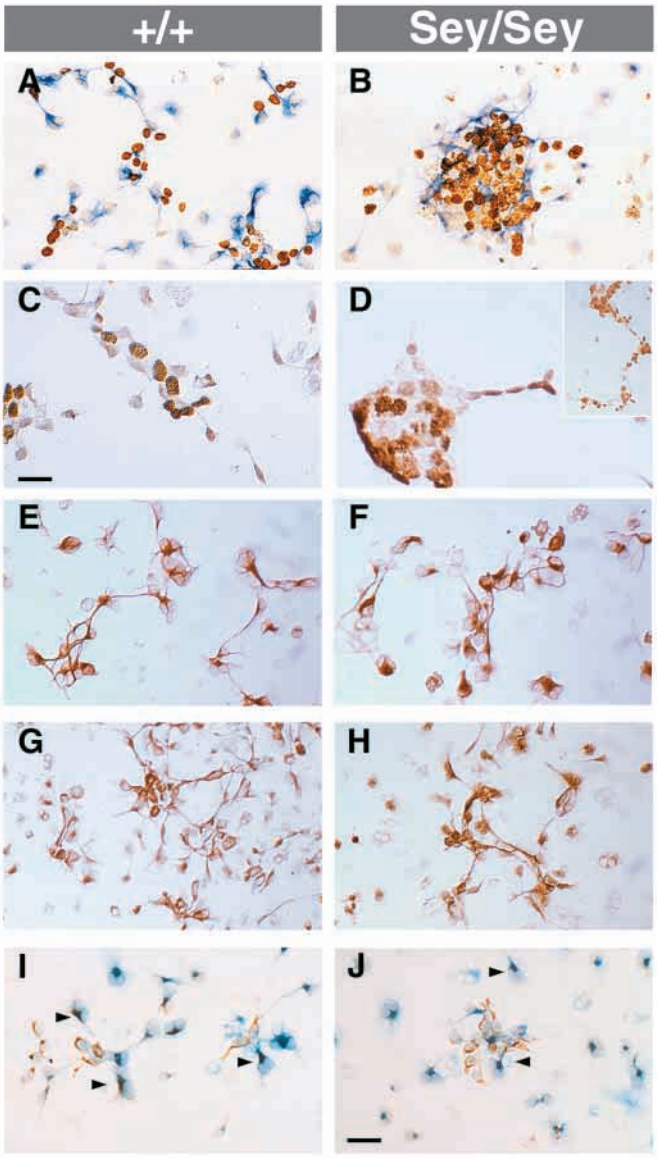

Fig. 6. Immunocytochemical analysis of dissociated cortical cells in culture. (A,C,E,G,I) Wild-type and (B,D,F,H,J) *Pax6*$^{Sey/Sey}$ dissociated cortical cells after 12.75 hours (E-J) and 24 hours (A-D) in culture. (A-D) BrdU labelling in cultures 24 hours after plating (11.25 hours after the end of the BrdU pulse). (A,B) Double immunostaining for BrdU (brown) and MAP2 (blue). In contrast to the wild-type BrdU-labelled cells, *Pax6*$^{Sey/Sey}$-labelled cells were mainly in large clusters. (C,D) Many mutant BrdU-labelled cells were grouped as to suggest cell-chain migration. Inset in D shows a panoramic view of mutant cortical cell-chain formation in culture. (E-J) Immunodetection of (E,F) neuronal antigen class III β tubulin (TuJ1), (G,H) nestin and (I,J) MAP2 (blue) and RC2 (brown). Arrowheads in I,J show cells expressing both markers. Scale bars: 24 μm in A,B,E-J; 16 μm in C,D.

In the cultures of wild-type cells, there were no significant changes in the percentages of cells expressing cyclin A (~20%) or p27^{Kip1} (~55%) between 12.75 and 24 hours after plating (Fig. 7C,D). In the cultures of *Pax6*$^{Sey/Sey}$ cells, the proportion of cells expressing cyclin A immediately after the pulse of BrdU was higher than in wild-type cultures (Fig. 7C), which is compatible with them having a higher proportion of BrdU-labelled cells at this time (Fig. 7A). Over the following 11.25 hours, the proportion of mutant cells expressing cyclin A decreased (Fig. 7C; $P<0.01$), whereas the proportion of mutant cells expressing p27^{Kip1} increased (Fig. 7D; $P<0.01$). This indicates that, unlike the wild-type cells, whose division maintains stable proportions of proliferating and postmitotic cells, division of the mutant cells is biased towards production of an ever-increasing proportion of postmitotic cells. This interpretation is illustrated in the schematic in Fig. 8.

DISCUSSION

Our main conclusions from in vivo work are that Pax6 is required in cortical development to regulate the rate of progression of progenitors through the cell cycle, the rate of progression from symmetrical to asymmetrical division and the onset of expression of neural-specific markers. In the absence of Pax6, the cell cycle and the onset of expression of neural-specific markers are both accelerated at the start of cortical neurogenesis. As neurogenesis progresses, the increase in the proportion of asymmetrical divisions occurs more rapidly than normal, and increasing proportions of progenitors divide in ectopic positions, suggesting that interkinetic nuclear migration becomes defective. By mid-neurogenesis, progenitor cell cycles in the mutant slow below the rate observed in wild-type embryos. We found that dissociated mutant cortical cells isolated in culture at E12.5 also showed more rapid proliferation and production of postmitotic cells than wild-type cells, suggesting that the changes seen in vivo are intrinsic to the cortical cells, rather than being secondary to one or more of the numerous extracortical defects in *Pax6*$^{Sey/Sey}$ embryos.

The differentiation of multipotential progenitor cells into

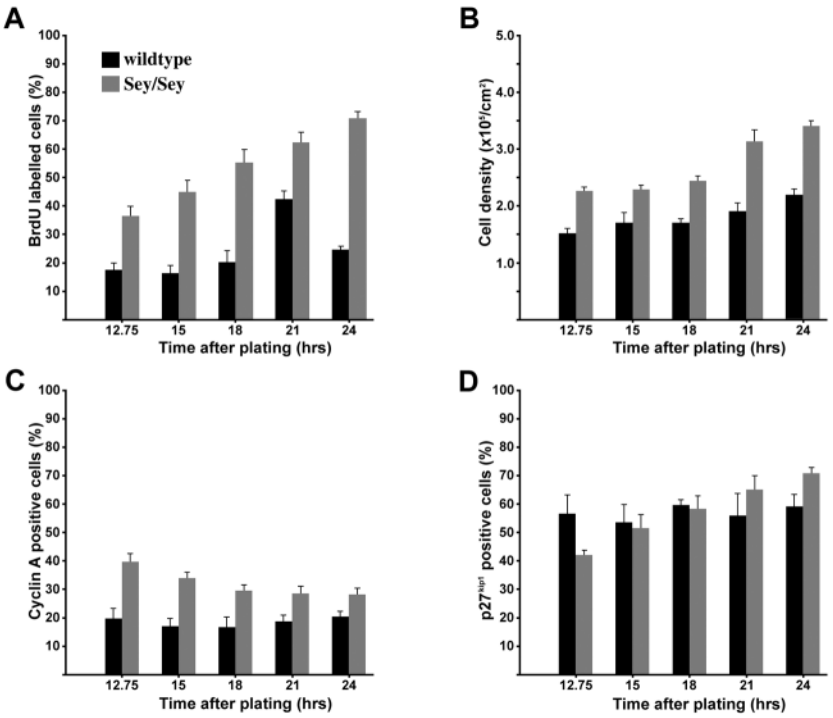

Fig. 7. Proliferation and differentiation in E12.5 wild-type and mutant dissociated cortical cell cultures between 12.75 and 24 hours after plating (all values are means±s.e.m.). (A) Percentages of BrdU-positive cells after a 45 minute pulse given 12 hours after plating. Significant differences (P<0.01) were observed between cultures of wild-type and mutant cells at all time-points from 12.75 hours after plating. (B) Cell density in cultures. Significant differences (P<0.01) were observed between cultures of wild-type and mutant cells at all time-points from 12.75 hours after plating. Regression analysis showed that the rate of increase for the mutant cells was just over twice that for the wild-type cells (r^2=0.88 for *Pax6*$^{Sey/Sey}$ and 0.99 for wild type). (C,D) Percentages of cells expressing cyclin A (C) and p27^{kip1} (D). Wild-type cells show no significant change in the number of cells expressing cyclin A and p27^{kip1} over the culture period (r^2=0.07 for wild-type data in C and 0.22 for wild-type data in D). There is a significant decrease in the percentage of mutant cells expressing cyclin A in culture (r^2=0.84). The percentages of *Pax6*$^{Sey/Sey}$ cells expressing p27^{kip1} increase with time (r^2=0.99).

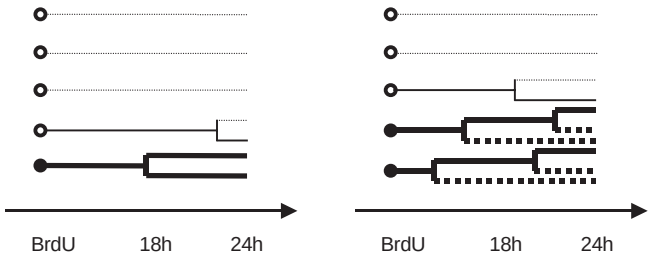

Fig. 8. Explanation of the most probable cause of the differences observed in the cultures (Fig. 7). (A) In wild-type cells, the data are compatible with cells having a cell-cycle time of around 12 hours, as has been shown previously in vivo (Takahashi et al., 1995b) (present study). Some cells are in S-phase during the 45 minute BrdU pulse and incorporate BrdU (filled circle); others will enter S-phase after the BrdU pulse or are postmitotic and will not label with BrdU (open circles). One in five cells are BrdU labelled following the pulse (i.e. 20%; compare with wild-type data at 12.75 hours in Fig. 7A). As the cells containing BrdU divide (thick lines), the proportion of BrdU-labelled cells in the culture increases. Once the nonlabelled cells divide (thin lines), the proportion of BrdU-labelled cells will decrease again. This trend is seen for wild-type data in Fig. 7A. Broken lines indicate cells that are postmitotic. Three in five cells are postmitotic at the time of the BrdU pulse (i.e. 60%; compare with wild-type data at 12.75 hours in Fig. 7D) and if half the divisions that occur in culture produce postmitotic neurones (shown as a broken line originating from the nonlabelled cell, although it could originate from the labelled cell), then roughly the same number will be postmitotic at 24 hours (four in seven cells, i.e. 57%; compare with wild-type data at 24 hours in Fig. 7D). The proportions of postmitotic cells and progenitor cells will not change greatly during culture in the scheme illustrated. (B) An interpretation of events in cultures of *Pax6*$^{Sey/Sey}$ cells is shown, using the same conventions as in A. A shorter cell cycle produces an initially higher proportion of BrdU-labelled cells (filled circles; two in five cells, or 40%; compare with data from mutants in Fig. 7A) and a subsequent steady increase in these proportions (four in seven cells at 18 hours; six in ten cells at 24 hours). This models the steady increase seen for mutant cells in Fig. 7A. The scheme illustrated, in which divisions produce one progenitor and one postmitotic cell, will lead to an abnormally rapid decrease in the proportions of progenitors and an increase in the proportions of postmitotic cells (from 40% at the time of the BrdU pulse to 70% at 24 hours; comparable with data from mutants in Fig. 7D).

specific classes of postmitotic neurones or glial cells occurs at characteristic times during neural development and appears to be accompanied by a progressive restriction of potential cell fate within the progenitors (Frantz and McConnell, 1996; Desai and McConnell, 2000). The regulation of this diversity requires a complex interaction between intracellular mechanisms and environmental cues. Clonal analysis on oligodendrocyte precursor cells suggests that an intrinsic clock operates within each cell to help control when it stops dividing and differentiates (Temple and Raff, 1986). It is probable that a similar internal clock, whose mechanism may be influenced by extracellular signals, acts to determine the rate of division and differentiation of neural progenitors. To date, however, little is known about the molecular mechanism that may govern such a clock. The results we present suggest that Pax6 may be an essential component.

During cortical neurogenesis in the wild-type telencephalon, the founder progenitor population undergoes a set number of 11 cell divisions (Takahashi et al., 1995b), during which there is a gradual switch from proliferative to neurogenic division (Takahashi et al., 1996). Coincident with this conversion is a decrease in the proportion of cells undergoing symmetrical divisions and an increase in the proportion undergoing asymmetrical divisions (Chenn and McConnnell, 1995). In this study, by comparing the orientations of mitotic spindles in *Pax6*$^{Sey/Sey}$ and wild-type cortex in vivo, we demonstrated a

more rapid progression to higher proportions of asymmetrical divisions in the absence of Pax6. This more rapid progression to asymmetrical division correlates with an accelerated production of cells expressing the markers Nbl and TuJ1. Both in wild-type and *Pax6*$^{Sey/Sey}$ cortex, therefore, circumstantial evidence suggests a link between the symmetry of cleavage and the production of postmitotic versus proliferative cells. Our in vitro work indicated that E12.5 *Pax6*$^{Sey/Sey}$ cortical cells retain the ability to proliferate more rapidly than normal and to generate increasing proportions of postmitotic cells even when dissociated and isolated in culture. This suggests that altered proliferation and differentiation in mutant cortical cells are not dependent on division taking place at an altered angle with respect to the ventricular surface, nor on the disruption to the interkinetic movement, neither of which would occur under these culture conditions. However, it cannot be ruled out that any intracellular reorganisation of cell fate determinants relative to the ventricular cycle has occurred prior to cell dissociation and that this memory is somehow retained within the dissociated cells for several cell cycles. Overall, our work does not allow us to draw firm conclusions on the nature of the relationship between cleavage plane and differentiation, i.e. whether they are causally related or independently regulated.

One parsimonious hypothesis to explain our various observations is as follows. Regulating the rate of progression through the cell cycle may be a primary function of Pax6 in early cortical progenitors. In the absence of Pax6, the cell cycle at E12.5 is shortened. If, in both wild-type and *Pax6*$^{Sey/Sey}$ embryos, the proportion of cells undergoing terminal differentiation is related to the number of cell cycles that a progenitor has gone through, rather than to the embryonic age of the cell in days, then an increase in the proportion of cells undergoing differentiation on a given day would follow as a consequence. Progenitors from an E12.5 *Pax6*$^{Sey/Sey}$ brain would be more advanced than those from an E12.5 wild-type brain in terms of their tendency to generate postmitotic cells, both in vivo and in vitro.

Intriguingly, examination of cell-cycle times at mid-neurogenesis (E15.5) showed that the absence of Pax6 produces a significantly slower cell cycle at this age. Even more surprisingly, the relative length of S phase has significantly increased in respect to the overall cell cycle. Previous work has indicated that, in contrast to cortical progenitors, diencephalic progenitors proliferate more slowly than normal in *Pax6*$^{Sey/Sey}$ embryos (Warren and Price, 1997). Therefore, it may be that, although a general function of Pax6 is to influence cell cycle times, the exact nature of its effect depends on the molecular and cellular context within which it acts. This context may change as the cortex develops. Another explanation, however, is that although the cells are cycling rapidly earlier on in development, there is insufficient time for all components essential for continued division to be synthesised and replenished. By E15.5, therefore, fundamental resources within the cells may be lost and the cell cycle may subsequently become deranged.

Throughout this study we did not find any evidence that changes in cell-cycle kinetics, proportions of asymmetrical divisions and rates of differentiation were different in different regions of the mutant cortex. Bishop et al. (Bishop et al., 2000) have suggested that an anterior-posterior gradient of *Pax6* expression contributes to regional differences in the differentiation of the cortex. It is possible, therefore, that *Pax6* regulates rates of proliferation and differentiation independently from any subsequent effects on the region-specific nature of the differentiation.

Although it is tempting to speculate on a single primary function for Pax6 in the cortex that can account for all the *Pax6*$^{Sey/Sey}$ cortical defects, in all probability Pax6 plays multiple roles. As a transcription factor, Pax6 may have distinct functions in different cells and at different times during development. Our data strongly suggest a cell cycle-related function, but it remains feasible that Pax6 has separate roles in regulating the cell cycle, cell differentiation and fate, cell adhesion and possibly other processes.

We thank K. Gillies, G. Grant and V. Allison for their technical help in this study, A.Carruthers and P. Teugue for help with statistics and P. Perry for help with imaging. Support was from the European Commission (BIOMED BMH4 CT97-2412 and TMR Programme, Marie Curie Research Training Grants ERB4001 GT972907) and BBSRC. G.E.-T is a Marie Curie Research Training Fellow and member of the Marie Curie Fellowship Association and P.R. is a Lister Research Fellow.

REFERENCES

Adams, R. J. (1996). Metaphase spindles rotate in the neuroepithelium of the rat cerebral cortex. *J. Neurosci.* **16**, 7610-7618.

Barres, B. A. (1999). A new role for glia: generation of neurons! *Cell* **97**, 667-670.

Bayer, S. A. and Altman, J. (1991). *Neocortical Development*. New York: Raven Press.

Bishop, K. M., Goudreau, G. and O'Leary, D. D. M. (2000). Regulation of area identity in the mammalian neocortex by Emx2 and Pax6. *Science* **288,** 344-349.

Bopp, D., Burri, M., Baumgartner, S., Frigerio, G. and Noll, M. (1986). Conservation of a large protein domain in the segmentation gene paired and in functionally related genes of *Drosophila*. *Cell* **47**, 1033-1040.

Borriello, A., Pietra, V. D., Criscuolo, M., Oliva, A., Tonini, G. P., Iolascon, A., Zappia, V. and Ragione, F. D. (2000). P27^{kip1} accumulation is associated with retinoic-induced neuroblastoma differentiation: evidence of decreased proteasome-dependent degradation. *Oncogene* **19**, 51-60.

Caric, D., Gooday, D., Hill, R. E., McConnell, S. K. and Price, D. J. (1997). Determination of the migratory capacity of embryonic cortical cells lacking the transcription factor *Pax-6*. *Development* **124**, 5087-5096.

Casaccia-Bonnefil, P., Tikoo, R., Kiyokawa, H., Friedrich, V., Jr, Chao, M. V. and Koff, A. (1997). Oligodendrocyte precursor differentiation is perturbed in the absence of the cyclin-dependent kinase inhibitor p27kip1. *Genes Dev*. **11**, 2335-2346.

Caviness, V. S., Jr, Takahashi, T. and Nowakowsky, R. S. (1995). Numbers, time and neocortical neurogenesis: a general developmental and evolutionary model. *Trends Neurosci.* **18**, 379-383.

Chenn, A. and McConnell, S. K. (1995). Cleavage orientation and the asymmetric inheritance of Notch 1 immunoreactivity in mammalian neurogenesis. *Cell* **82**, 631-641.

Dahl, D. (1981). The vimentin-GFAP protein transition in rat neuroglia cytoskeleton occurs at the time of myelination. *J. Neurosci. Res.* **6**, 741-748.

Darzynkiewicz, Z., Gong, J., Juan, G., Ardelt, B. and Traganos, F. (1996). Cytometry of cyclin proteins. *Cytometry* **25**, 1-13.

Desai, A. R. and McConnell, S. K. (2000). Progressive restriction in fate potential by neural progenitors during cerebral cortical development. *Development* **127**, 2863-2872.

Doe, C. Q. (1996). Asymmetrical cell division and neurogenesis. *Curr. Opin. Genet. Dev.* **6**, 562-566.

Durand, B., Gao, F. B. and Raff, M. (1997). Accumulation of the cyclin-dependent kinase inhibitor p27/kip1 and the timing of oligodendrocyte differentiation. *EMBO J.* **16**, 306-317.

Durand, B., Fero, M. L., Roberts, J. M. and Raff, M. (1998). P27^{kip1} alters the response of cells to mitogen and is part of the cell-intrinsic timer that arrests the cell cycle and initiates differentiation. *Curr. Biol.* **8**, 431-440.

Easter, S. S., Ross, L. S. and Franfurter, A. (1993). Initial tract formation in the mouse brain. *J. Neurosci*. **13**, 285-299.

Frantz, G. D. and McConnell, S. K. (1996). Restriction of late cerebral cortical progenitors to an upper-layer fate. *Neuron* **17**, 55-61.

Frigerio, G., Burri, M., Bopp, D., Baumgartner, S. and Noll, M. (1986). Structure of the segmentation gene paired and the *Drosophila* PRD gene set as part of a gene network. *Cell* **47**, 735-746.

Fujita, S. (1964). Analysis of neuron differentiation in the central nervous system by tritiated thymidine autoradiography. *J. Comp. Neurol.* **122**, 311-328.

Gillies, K. and Price, D. J. (1993). The fates of cells in the developing cerebral cortex of normal and methylazoxymethanol acetate-lesioned mice. *Eur. J. Neurosci*. **5**, 73-84.

Götz, M., Stoykova, A. and Gruss, P. (1998). *Pax6* controls radial glia differentiation in the cerebral cortex. *Neuron* **21**, 1031-1044.

Grindley, J. C., Davidson, D. R. and Hill, R. E. (1995). The role of *Pax6* in eye and nasal development. *Development* **121**, 1433-1442.

Grindley, J. C., Hargett, L., Hill, R. E., Ross, A. and Hogan, B. L. M. (1997). Disruption of *Pax6* function in mice homozygous for the *Pax6$^{Sey\text{-}Neu}$* mutation produces abnormalities in the early development and regionalization of the diencephalon. *Mech. Dev.* **64**, 111-126.

Grove, E. A., Williams, B. P., Li, D. Q., Hajihosseini, M., Friedrich, A. and Price, J. (1993). Multiple restricted lineages in the embryonic rat cerebral cortex. *Development* **117**, 553-561.

Hendzel, M. J., Wei, Y., Mancini, M. A., van Hooser, A., Ranalli, T., Brinkley, B. R., Bazett-Jones, D. P. and Allis, C. D. (1997). Mitosis-specific phosphorylation of histone H3 initiates primarily within pericentromeric heterochromatin during G2 and spreads in an ordered fashion coincident with mitotic chromosome condensation. *Chromosoma* **106**, 348-360.

Hill, R. E., Favor, J., Hogan, B. M. L., Ton, C. C. T., Saunders, G. F., Hanson, I. M., Prosser, J., Jordan, T., Hastie, N. D. and van Heyningen, V. (1991). Mouse small eye results from mutation in a paired-like homeobox-containing gene. *Nature* **354,** 522-525.

Hogan, B. M. L., Horsnurgh, G., Cohen, J., Hetherington, C. M., Fischer, G. and Lyon, M. F. (1986). Small eye (*Sey*): a homozygous lethal mutation on chromosome 2 which affects the differentiation of both lens and nasal placodes in the mouse. *J. Embryol. Exp. Morphol.* **97**, 95-110.

Kawakami, A., Kinura-Kawakami, M., Nomura, T. and Fujisawa, H. (1997). Distributions of PAX6 and PAX7 proteins suggest their involvement in both early and late phases of chick brain development. *Mech. Dev.* **66**, 119-130.

Kornack, D. R. and Rakic, P. (1995). Radial and horizontal deployment of clonally related cells in the primate neocortex: relationship to distinct mitotic lineages. *Neuron* **15**, 311-321.

Lee, M. K., Tuttle, J. B., Rebhun, L. L., Cleveland, D. W. and Frankfurter, A. (1990). The expression and posttranslational modification of a neuron-specific β-tubulin isotype during chick embryogenesis. *Cell Motil. Cytoskel.* **17**, 118-132.

Lendahl, U., Zimmerman, L. B. and McKay, R. D. (1990). CNS stem cell express a new class of intermediate filament protein. *Cell* **60**, 585-595.

Levine, E. M., Close, J., Fero, M., Ostrovsky, A. and Reh, T. A. (2000). P27kip1 regulates cell cycle withdrawal of late multipotent progenitor cells in the mammalian retina. *Dev. Biol.* **219**, 299-314.

Lu, B., Jan, L. and Jan, Y. N. (2000). Control of cell divisions in the nervous system: symmetry and asymmetry. *Ann. Rev. Neurosci.* **23**, 531-556.

Luskin, M. B., Pearlman, A. L. and Sanes, J. R. (1988). Cell lineage in the cerebral cortex of the mouse studied in vivo and in vitro with a recombinant retrovirus. *Neuron* **1**, 635-647.

Malatesta, P., Hartfuss, E. and Gotz, M. (2000). Isolation of radial glial cells by fluorescence-activated cell sorting reveals a neuronal lineage. *Development* **127**, 5253-5263.

Marín-Padilla, M. (1998). Cajal-Retzius cells and the development of the neocortex. *Trends Neurosci.* **21**, 64-71.

Mastick, G. S., Davis, N. M., Andrews, G. L. and Easter, S. S., Jr (1997). *Pax6* functions in boundary formation and axon guidance in the embryonic mouse forebrain. *Development* **124**, 1985-1997.

Matsuzaki, F. (2000). Asymmetric division of *Drosophila* neural stem cells: a basis for neural diversity. *Curr. Opin. Neurol*. **10**, 38-44.

Matus, A. (1991). Microtubule associated proteins and neuronal morphogenesis. *J. Cell Sci.* (Suppl.) **15**, 61-67.

Mione, M. C., Cavanagh, J. F. R., Harris, B. and Parnavelas, J. G. (1997). Cell fate specification and symmetrical/asymmetrical divisions in the developing cerebral cortex. *J. Neurosci.* **17**, 2018-2029.

Misson, J. P., Edwards, M. A., Yamamoto, M. and Caviness, V. S., Jr (1988). Identification of the radial glial cells within the developing murine cerebral nervous system: studies based upon a new immunohistochemical marker. *Dev. Brain Res.* **44**, 95-108.

Miyazawa, K., Himi, T., Garcia, V., Yamagishi, H., Sato, S. and Ishizaki, Y. (2000). A role for p27/kip1 in the control of cerebellar granule cell precursor proliferation. *J. Neurosci*. **20**, 5756-5763.

Nowakowski, R. S., Lewin, S. B and Miller, M. W. (1989) Bromodeoxyuridine immunohistochemical determination of the lengths of the cell cycle and the DNA-synthetic phase for an anatomically defined population. *J. Neurocytol.* **18,** 311-318.

Price, J. and Thurlow, L. (1988). Cell lineage in the rat cerebral cortex: a study using retroviral-mediated gene transfer. *Development* **104**, 473-482.

Price, D. J., Aslam, S., Tasker, L. and Gillies, K. (1997). Fates of the earliest generated cells in the developing murine neocortex. *J. Comp. Neurol.* **377**, 414-422.

Qian, X., Goderie, S. K., Shen, Q., Stern, J. S. and Temple, S. (1998). Intrinsic programs of patterned cell lineages in isolated vertebrate CNS ventricular zone cells. *Development* **125**, 3143-3152.

Reid, C. B., Liang, I. and Walsh, C. (1995). Systematic widespread clonal organization in cerebral cortex. *Neuron* **15**, 299-310.

Roberts, R. C. (1967). *Small-eyes*, a new dominant mutant in the mouse. *Genet. Res*. **9**, 121-122.

Romijn, H. J., Vanhuizen, F. and Wolters, P. S. (1994). Towards an improved serum-free, chemically defined medium for long-term culturing of cerebral cortex tissue. *Neurosci. Biobehav. Rev.* **8**, 301-334.

Sasaki, K., Tamura, S., Tachibana, H., Sugita, M., Gao, Y., Furuyama, J. I., Kakishita, E., Sakai, T., Tamaoki, T. and Tamaoki, T. H. (2000). Expression and role of p27^{kip1} in neuronal differentiation of embryonal carcinoma cells. *Mol. Brain Res.* **77**, 209-221.

Sauer, F. C. (1935). Mitosis in the neural tube. *J. Comp. Neurol.* **286**, 442-455.

Schmahl, W., Knoediseder, M., Favor, J. and Davidson, D. (1993). Defects of neural migration and the pathogenesis of cortical malformations are associated with small eye (*sey*) in mouse, a point mutation at the *Pax-6* locus. *Acta Neuropathol*. **86**, 126-135.

Sherr, C. J. and Roberts, J. M. (1995). Inhibitors of mammalian G1 cyclin-dependent kinases. *Genes Dev.* **9**, 1149-1163.

Sherr, C. J. and Roberts, J. M. (1999). CDK inhibitors: positive and negative regulators of G1-phase progression. *Genes Dev.* **13**, 1501-1512.

Shetty, A. K. and Turner, D. A. (1998). In vitro survival and differentiation of neurons derived from epidermal growth factor-responsive postnatal hippocampal stem cells: inducing effects of brain-derived neurotrophic factor. *J. Neurobiol.* **35**, 395-425.

Sidman, R. L., Miale, I. L. and Feder, N. (1959). Cell proliferation and migration in the primitive ependymal zone: an autoradiographic study of histogenesis in the nervous system. *Exp. Neurol.* **1**, 322-333.

Sprinkle, T. J., Agee, J. F., Tippins, R. B., Chaberlain, C. R., Faguet, G. B. and De Vries, G. H. (1987). Monoclonal antibody production to human and bovine 2′:3′-cyclic nucleotide 3′-phosphodiesterase (CNPase): high-specificity recognition in whole brain acetone powders and conservation of sequence between CNP1 and CNP2. *Brain Res.* **426**, 349-357.

Stoykova, A. and Gruss, P. (1994). Roles of Pax-genes in developing and adult brain as suggested by expression patterns. *J. Neurosci*. **14**, 1395-1412.

Stoykova, A., Fritsch, R., Walther, C. and Gruss, P. (1996). Forebrain patterning defects in Small eye mutant mice. *Development* **122**, 3453-3465.

Takahashi, T., Nowakowski, R. S. and Caviness, V. S., Jr (1993). Cell cycle parameters and patterns of nuclear movement in the neocortical proliferative zone of the fetal mouse. *J. Neurosci.* **13**, 820-833.

Takahashi, T., Nowakowski, R. S. and Caviness, V. S., Jr (1995a). Early ontogeny of the secondary proliferative population of the embryonic murine cerebral wall. *J. Neurosci.* **15**, 6058-6068.

Takahashi, T., Nowakowski, R. S. and Caviness, V. S., Jr (1995b). The cell cycle of the pseudostratified ventricular epithelium of the embryonic murine cerebral wall. *J. Neurosci.* **15**, 6046-6057.

Takahashi, T., Nowakovski, R. S. and Caviness, V. S., Jr (1996). Interkinetic and migratory behaviour of a cohort of neocortical neurons arising in the early embryonic murine cerebral wall. *J. Neurosci*. **16**, 5762-5776.

Temple, S. and Raff, M. (1986). Clonal analysis of oligodendrocyte development in culture: evidence for a developmental clock that counts cell divisions. *Cell* **44**, 773-779.

Temple, S. and Davis, A. A. (1994). Isolated rat cortical progenitor cells are maintained in division in vitro by membrane-associated factors. *Development* **120**, 999-1008.

Treisman, F., Harris, E. and Desplan, C. (1991). The paired box encodes a second DNA-binding domain in the paired homeodomain protein. *Genes Dev.* **5**, 594-604.

Walsh, C. and Cepko, C. L. (1992). Widespread dispersion of neuronal clones across functional regions of the cerebral cortex. *Science* **255**, 434-440.

Walther, C. and Gruss, P. (1991). *Pax-6*, a murine paired box gene, is expressed in the developing CNS. *Development* **113**, 1435-1449.

Warren, N. and Price, D. J. (1997). Roles of *Pax6* in murine diencephalic development. *Development* **124**, 1573-1582.

Warren, N., Caric, D., Pratt, T., Clausen, J. A., Asavaritikrai, P., Mason, J. O., Hill, R. E. and Price, D. J. (1999). The transcription factor, *Pax6*, is required for cell proliferation and differentiation in the developing cerebral cortex. *Cereb. Cortex* **9**, 627-635.

Williams, B. P. and Price, J. (1995). Evidence for multiple precursor cell types in the embryonic rat cerebral cortex. *Neuron* **14**, 1181-1188.

Zhong, W., Feder, J. N., Jiang, M. M., Jan, L. Y. and Jan, Y. N. (1996). Asymmetrical localization of a mammalian Numb homolog during mouse cortical neurogenesis. *Neuron* **17**, 43-53.

Zhong, W., Jiang, M. M., Weinmaster, G., Jan, L. Y. and Jan, Y. N. (1997). Differential expression of mammalian Numb, Numblike and Notch1 suggests distinct roles during mouse cortical neurogenesis. *Development* **124**, 1887-1897.